ELSEVIER

Journal of Hydrology 166 (1995) 461–478

Journal of Hydrology

[3]

Distributed estimation of incoming direct solar radiation over a drainage basin

Roberto Ranzi[a,*], Renzo Rosso[b]

[a]*Department of Civil Engineering, Università di Brescia, Via Branze 38, I-25123 Brescia, Italy*
[b]*Department of Hydraulic Environmental and Surveying Engineering, Politecnico di Milano, Piazza Leonardo da Vinci 32, I-20133 Milan, Italy*

Received 16 August 1993; accepted 1 July 1994

Abstract

Because of topographic variability, the global flux of incoming direct solar radiation over a drainage basin of high relief should be evaluated by grid modelling. Alternatively, line integration throughout the catchment boundary can be substituted for areal integration over the detailed three-dimensional representation of basin topography. This method is based on the Stokes' theorem and it yields a general and efficient solution, which can also account for shadowing effects. Application to three small mountainous catchments is reported for varying solar geometry and the performance of a lumped model is also examined. The approach can be applied to estimate the contribution of shortwave radiative fluxes to the processes of snowmelt and evapotranspiration at the basin scale.

1. Introduction

Solar radiation is a key factor in most surface climate processes. In surface basin hydrology, it controls the energy balance of the catchment, thus deeply influencing the water balance. In the solar spectrum, terrain slopes are irradiated from three sources; these are: diffuse irradiance from the sky, direct and diffuse irradiance reflected from nearby terrain, and direct irradiance from the Sun, which will be examined in the present paper. Estimates of clear-sky direct solar radiation are required in many climatic and hydrological studies, because the flux of incoming direct radiation over a drainage basin is the controlling factor of fundamental hydrological processes at the land–atmosphere interface, such as evapotranspiration and

* Corresponding author.

SSDI 0022-1694(94)05099-6

snowmelt. Because this flux must be modelled for a given portion of terrain on the Earth's surface, i.e. a drainage basin, it must be understood how clear-sky solar radiation operating at scale of micrometers integrates upward to affect interactions at hydrological scales of tens of metres to tens of kilometres (see Wood et al., 1988).

While seasonal and latitudinal variations are well understood and described, only recent studies analysed topographic variability in diurnal and seasonal radiation patterns over a region or locally (Williams et al., 1972; Holland and Steyn, 1975; Dozier and Outcalt, 1979; Dozier, 1980; Kirkpatrick and Nunez, 1980; Dubayah et al., 1989; Isard, 1983). These studies pointed out that spatial and temporal variations in radiation are fundamental to understanding remotely sensed data on surface hydrology because significant spatiotemporal variability occurs at scales below and above the resolution of airborne and satellite-borne sensors (Mancini et al., 1993). Accordingly, areal estimation of the global flux owing to incoming clear-sky direct radiation over a catchment must also account for spatial variability. For the purpose, the increasing availability of Geographical Information Systems allows for the automated use of topographic data to investigate spatially variable hydrological processes (see Burrough, 1986; Band, 1989). Although different methods can be used to build Digital Elevation Models (DEMs) for hydrological studies (e.g. rectangular grid networks, triangular irregular networks and contour-based networks), grid structures provide the best compromise between accuracy and computational efficiency (Moore et al., 1991). Therefore, distributed modelling of solar radiation on topographic grids can describe the effects of terrain configuration by using a detailed three-dimensional representation of topography in order to integrate the local vector representing direct solar radiation (Ranzi and Rosso, 1991).

However, modelling of solar radiation on topographic grids could result in a rather cumbersome exercise, because of the availability and cost of digital elevation data at fine grid spacing, let alone the computational effort. To overcome this problem, Dubayah et al. (1990) studied the interaction between solar geometry and topography, and reported a lumped model of solar radiation based on a probabilistic description of the major features of terrain configuration. Nevertheless, this approach may still involve a degree of approximation, because the assumptions underlying the simplified terrain configuration can yield a more or less effective representation of real topography. Therefore, searching for an alternative, but analytical, solution is of interest to hydrological applications.

The present paper deals with the distributed evaluation of the incoming global direct radiative flux over a basin by using different methods. In the following section, grid estimation is reviewed briefly, and a technique to account for the effects of topographic shadowing is reported. An alternative approach based on the application of the Stokes' formula is presented in the third section. This approach provides a simple and efficient solution for mountainous terrain; it is also capable of accounting for shadowing effects, as shown in the fourth section. A discussion of the effects of shadow provides a better insight into the Stokesian approach, following an original idea introduced by Ranzi and Rosso (1993). Application for three small mountainous catchments is presented in the fifth section, and the performance

of the lumped approach of Dubayah et al. (1990) is compared with that of the distributed approach.

2. Grid estimation of direct solar radiation

At a given time, t, and location on the Earth's surface, $\boldsymbol{x}$, clear-sky direct radiation from the Sun can be represented by a three-dimensional vector field, say $\boldsymbol{I}(\boldsymbol{x}, t)$, where $\boldsymbol{x} = \{x_1, x_2, x_3\}$ denotes a point in R^3, x_1 and x_2 being its horizontal coordinates, and x_3 the vertical one (see Fig. 1). Denoting with $I(t)$ the intensity of direct irradiance from the Sun, the three components of $\boldsymbol{I}(\boldsymbol{u}, t)$ along the three axes can be given as

$$I_1(\boldsymbol{u}, t) = -I(t) \cos h(\boldsymbol{u}, t) \cos \pi(\boldsymbol{u}, t) \tag{1a}$$

$$I_2(\boldsymbol{u}, t) = I(t) \cos h(\boldsymbol{u}, t) \sin \pi(\boldsymbol{u}, t) \tag{1b}$$

$$I_3(\boldsymbol{u}, t) = I(t) \sin h(\boldsymbol{u}, t) \tag{1c}$$

respectively, where $h(\boldsymbol{u}, t)$ denotes the temporal function representing the solar altitude angle for site $\boldsymbol{u}$, and $\pi(\boldsymbol{u}, t)$ that representing the solar azimuth angle measured with respect to the north. Accordingly, $\boldsymbol{I}(\boldsymbol{u}, t)$ depends on solar geometry for the site under examination. Although direct irradiance from the Sun is a physical process operating at the scale of micrometres, its spatial variability can be neglected; therefore, $h(\boldsymbol{u}, t) \equiv h(t)$, and $\pi(\boldsymbol{u}, t) \equiv \pi(t)$ yield $\boldsymbol{I}(\boldsymbol{u}, t) \equiv \boldsymbol{I}(t)$. In the following this situation, which occurs for a wide range of spatial scales of hydrological interest, will be investigated.

Let $A(\boldsymbol{x})$ denote the three-dimensional function representing the topographic configuration of the drainage basin under examination. The global flux of clear-sky incoming radiation over the basin surface must be evaluated by integrating the incoming radiation over $A(\boldsymbol{x})$. Accordingly, the average flux over the basin surface at time t is given by

$$\Phi_A(t) = \frac{1}{A_*} \iint_{A(\boldsymbol{x})} \boldsymbol{I}(t) \cdot \boldsymbol{N}_{A(\boldsymbol{x})} \mathrm{d}A(\boldsymbol{x}) \tag{2}$$

where $\boldsymbol{N}_{A(\boldsymbol{x})}$ denotes the unit vector of the principal normal to surface $A(\boldsymbol{x})$, A_* the surface area as projected on the horizontal plane, and $\cdot$ the operator of scalar product. When digital elevation data at fine grid spacing are available for the basin, generally in raster form by DEMs, integration of (2) can be carried out by finite summation of the contributions by each grid point. For the purpose, the local interaction between topography and solar geometry must be determined for each pixel by grid evaluation of the scalar product between $\boldsymbol{I}(t)$ and $\boldsymbol{N}_{A(\boldsymbol{x})}$ (Band, 1993).

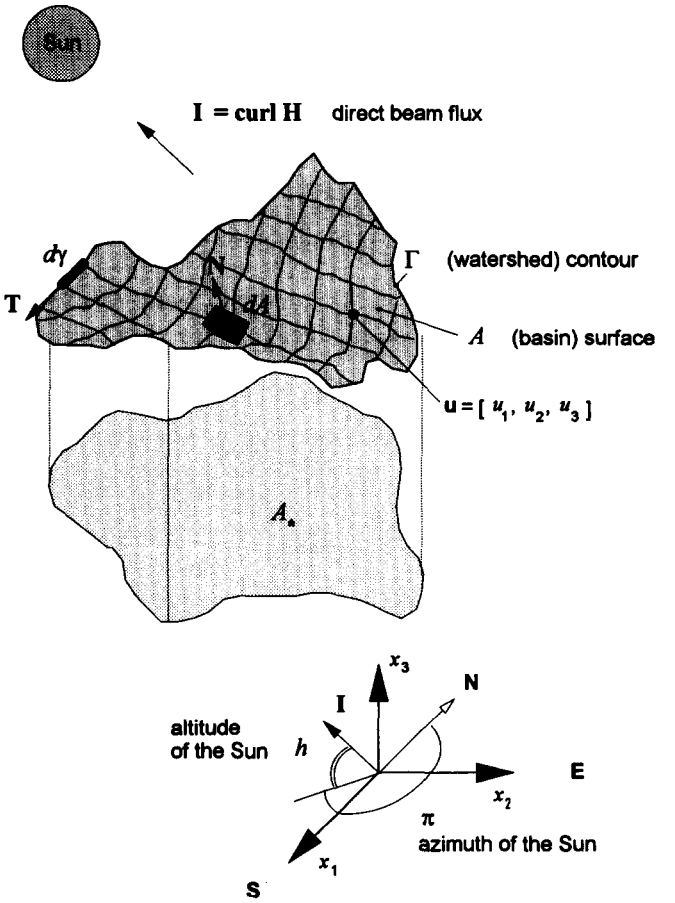

Fig. 1. Sketch of clear-sky incoming direct radiation process over a drainage basin.

The accuracy of this computation is obviously related to the resolution of the available DEM for the area being examined.

In drainage basins of high relief shadowing of some areas can occur for low solar altitudes (see Fig. 2). Accordingly, for any location $\boldsymbol{u}$ of the basin, the effective irradiance vector, $\boldsymbol{I}_e(\boldsymbol{u}, t)$, must be written as

$$\boldsymbol{I}_e(\boldsymbol{u}, t) = \begin{cases} \boldsymbol{I}(\boldsymbol{u}, t), & \text{for } \boldsymbol{u} \notin A_0(\boldsymbol{x}, t) \\ \boldsymbol{0}, & \text{for } \boldsymbol{u} \in A_0(\boldsymbol{x}, t) \end{cases} \tag{3}$$

where $A_0(\boldsymbol{x}, t)$ denotes the shaded portion of the basin surface, $A(\boldsymbol{x})$. It must be noticed that the shaded area of the basin surface is a spatio-temporal function, because it depends on both topography and solar geometry. The average flux of incoming direct solar radiation over the basin surface at time t is still given by (2),

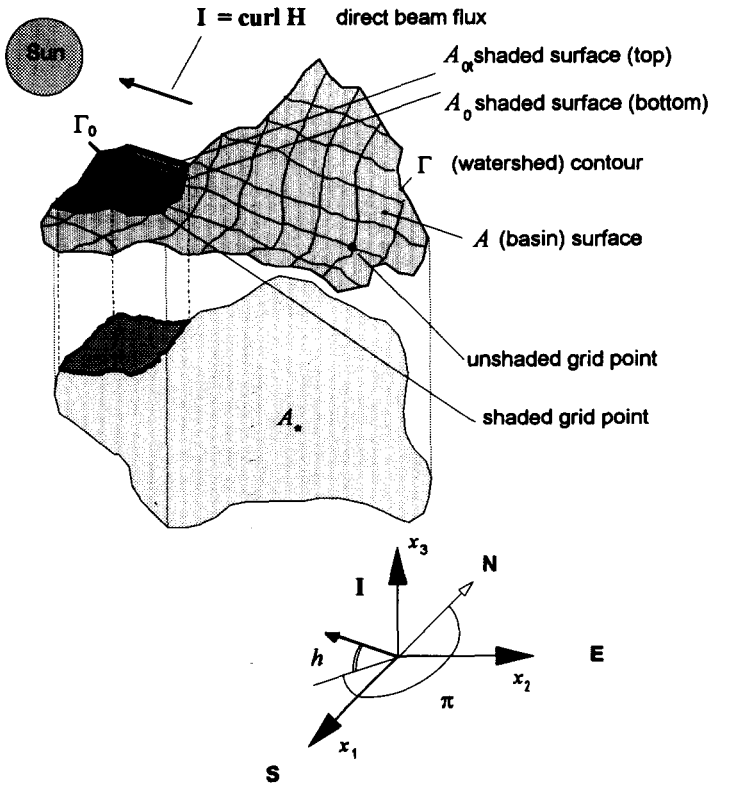

Fig. 2. Sketch of shadowing effects on clear-sky incoming direct radiation process over a drainage basin.

but $\boldsymbol{I}_e(\boldsymbol{u}, t)$ must be substituted for $\boldsymbol{I}(t)$, thus obtaining

$$\Phi_A(t) = \frac{1}{A_*} \iint_{A(x)} \boldsymbol{I}_e(\boldsymbol{x}, t) \cdot \boldsymbol{N}_{A(x)} \mathrm{d}A(\boldsymbol{x}). \tag{4}$$

Grid modelling can be applied to solve the integral on the right-hand side of (4) when digital elevation data at fine grid spacing are available for the basin. For given solar geometry, the grid points must be pre-processed to identify the shaded pixels. Then, integration of (4) can be carried out by finite summation of the non-zero contributions by each grid point, which is finally normalised by the total number of grid points.

3. The Stokesian method

3.1. Theory

Because $\boldsymbol{I}(t)$ is a solenoidal vector field in R^3, it can be written as

$$\boldsymbol{I}(t) = \nabla \times \boldsymbol{H}(t), \tag{5}$$

where $\times$ denotes the operator of vector product, and $\nabla \times \boldsymbol{H}$ is the rotation (curl) of a vector field $\boldsymbol{H}$, the components of which are given by

$$H_1(t) = x_3 I_2(t) \tag{6a}$$

$$H_2(t) = x_1 I_3(t) \tag{6b}$$

$$H_3(t) = x_2 I_1(t) \tag{6c}$$

respectively. Accordingly, the components of $\boldsymbol{I}(t)$ are written as

$$I_1(t) = \frac{\partial H_3(t)}{\partial x_2} - \frac{\partial H_2(t)}{\partial x_3} \tag{7a}$$

$$I_2(t) = \frac{\partial H_1(t)}{\partial x_3} - \frac{\partial H_3(t)}{\partial x_1} \tag{7b}$$

$$I_3(t) = \frac{\partial H_2(t)}{\partial x_1} - \frac{\partial H_1(t)}{\partial x_2} \tag{7c}$$

where $\partial H_i / \partial H_j$ is the first partial derivative of the ith component of $\boldsymbol{H}(t)$ with respect to the jth axis. Under weak mathematical restrictions (i.e. $A(\boldsymbol{x})$ must be continuous with continuous derivatives up to the second order, and bounded by a closed contour) one can apply the Stokes' formula (see Demidovich, 1968, p. 285) to solve the surface integral on the right-hand side of (2). The result is given by

$$\Phi_A(t) = \frac{1}{A_*} \oint \boldsymbol{H}(t) \cdot \boldsymbol{T}_\gamma \mathrm{d}\gamma, \tag{8}$$

where Γ denotes the contour of the surface examined, i.e. the catchment boundary, $\boldsymbol{T}_\gamma$ the unit vector of the tangent line to Γ, γ the curvilinear coordinate, and $\cdot$ the scalar product (see Fig. 1). Because using (8) instead of (2) involves the computation of a line integral instead of a surface one, (8) can provide more straightforward estimates of areal radiation than those achievable by using (2) without any loss of accuracy. Moreover, (8) can be also rearranged as follows to obtain a simple, and meaningful formulation of the solution of the problem.

3.2. Solution neglecting shadowing effects

Let $\boldsymbol{R}(t)$ denote the vector with components

$$R_1(t) = I_2(t) = I(t) \cos h(t) \sin \pi(t) \tag{9a}$$

$$R_2(t) = I_3(t) = I(t) \sin h(t) \tag{9b}$$

$$R_3(t) = I_1(t) = -I(t) \cos h(t) \cos \pi(t) \tag{9c}$$

which is obtained from $\boldsymbol{I}(t)$ simply by shifting its components. Further, let $\boldsymbol{B}$ denote

the vector with components

$$B_1 = \frac{1}{A_*} \oint_{\Gamma} x_3 T_{1\gamma} \, d\gamma \tag{10a}$$

$$B_2 = \frac{1}{A_*} \oint_{\Gamma} x_1 T_{2\gamma} \, d\gamma \tag{10b}$$

$$B_3 = \frac{1}{A_*} \oint_{\Gamma} x_2 T_{3\gamma} \, d\gamma \tag{10c}$$

where $T_{1\gamma}$, $T_{2\gamma}$ and $T_{3\gamma}$ denote the components of $\boldsymbol{T}_\gamma$ along the three axes, x_1, x_2 and x_3, respectively. Accordingly, (8) can be written as

$$\Phi_A(t) = \boldsymbol{B} \cdot \boldsymbol{R}(t), \tag{11}$$

where $\boldsymbol{R}(t)$ is defined as the 'shifted beam radiation' vector, which depends on solar altitude and azimuth, and $\boldsymbol{B}$ as the 'topographic boundary' vector, which is dimensionless and depends on the configuration of the terrain of the basin. Thus, clear-sky incoming direct radiation over the area examined can be estimated from the scalar product of two vectors, the first, $\boldsymbol{R}(t)$, depending on solar geometry, and the second, $\boldsymbol{B}$, on catchment topography. Moreover, (11) accounts separately for the temporal and spatial variability of direct solar radiation, because $\boldsymbol{R}(t)$ depends on daily and seasonal variations of solar geometry, and $\boldsymbol{B}$ on the configuration of the terrain as represented by the catchment boundary. This latter can be considered as the parameter vector which lumps the effects of topography on incoming direct solar radiation over a drainage basin.

4. Shadowing effects

When shadowing is considered, the effective irradiance, $\boldsymbol{I}_e(\boldsymbol{x}, t)$, is no longer a solenoidal vector field with reference to $A(\boldsymbol{x})$. However, the effective average basin flux, $\Phi_{A_e}(t)$ can be still evaluated by the Stokesian approach, because it can be written as

$$\Phi_{A_e}(t) = \Phi_A(t) - \Phi_{A_0}(t) \tag{12}$$

where $\Phi_{A_0}(t)$, the flux of the direct irradiance vector over the shaded area, is given by

$$\Phi_{A_0}(t) = \frac{1}{A_*} \int_{A_0(\boldsymbol{x})} \boldsymbol{I}(t) \cdot \boldsymbol{N}_{A(\boldsymbol{x})} dA = \frac{1}{A_*} \oint_{\Gamma_0} \boldsymbol{H}(t) \cdot \boldsymbol{T}_\gamma \, d\gamma \tag{13}$$

with $\Gamma_0 = \Gamma_0(t)$ denoting the contour of the shaded areas, which results in a temporal function (see Fig. 2). The solution of (12) can be carried out formally as above,

because (12) can be rearranged in the form

$$\Phi_A(t) = [\boldsymbol{B} - \boldsymbol{B}_0(t)] \cdot \boldsymbol{R}(t) \tag{14}$$

where $\boldsymbol{R}(t)$ is the 'shifted beam radiation' vector depending on solar geometry, $\boldsymbol{B}$ is the 'topographic boundary' vector depending on the boundary of the catchment, and $\boldsymbol{B}_0(t)$ is the 'shaded areas topographic boundary' vector, the components of which are given by

$$B_{01} = \frac{1}{A_*} \oint_{\Gamma_0(t)} x_3 T_{1\gamma} \mathrm{d}\gamma \tag{15a}$$

$$B_{02} = \frac{1}{A_*} \oint_{\Gamma_0(t)} x_1 T_{2\gamma} \mathrm{d}\gamma \tag{15b}$$

$$B_{03} = \frac{1}{A_*} \oint_{\Gamma_0(t)} x_2 T_{3\gamma} \mathrm{d}\gamma \tag{15c}$$

It must be noticed that $\boldsymbol{B}_0(t)$ does not lump basin topography, but it depends on both basin topography and solar geometry. Therefore, the Stokesian solution accounting for shadowing effects can be much more cumbersome than the previous one, which neglects these effects, because the application of (14) is rather less straightforward than that of (11). Moreover, because several shaded areas may occur in the basin, the integrals of (15) could involve the sum of all these contributions. However, it must be observed that shadowing generally occurs for solar altitude less than 20°–30°, when direct radiation is less important in relation to the other radiative fluxes, i.e. diffuse irradiance from the sky, and direct and diffuse irradiance reflected from nearby terrain.

4.1. Self-shadowing catchments

A further property of solenoidal vector fields can be used to show that (11) still remains strictly correct also when topographic shadow occurs over the basin surface, in many cases. For the purpose one must introduce the concept of 'self-shadowing catchment'. A catchment is 'self-shadowing' when two conditions holds. First, the shadow occurring over the basin surface must be projected from a horizon line which belongs to the catchment itself, and not from other topographic features, such as mountains or hills, beyond the boundary of the catchment. Second, the shadow projected from the basin surface, if any occurs, must fall within the basin area.

Under these circumstances one can show that Eq. (11) still holds. Let the closed surface, S_0, be constructed by covering the shaded area, A_0, with a surface, denoted by A_{0t}, which is tangential to the direct beam flux (see Fig. 2). Since the flux of a

solenoidal vector field through a closed surface is nil, one gets

$$\Phi_{S_0}(t) = \frac{1}{A_*} \oiint_{S_0(x)} \boldsymbol{I}(t) \cdot \boldsymbol{N}_{S(x)} \, \mathrm{d}S = 0 \tag{16}$$

where $\Phi_{S_0(t)}$ is the flux of $\boldsymbol{I}$ through S_0. If the basin is self-shadowing, the surface S_0 is partitioned by the contour Γ_0 into two parts, say the bottom, A_0, and the top, A_{0t}, and the flux through S_0 is given by the sum of the fluxes through these two surfaces. The flux through the covering part, A_{0t}, is nil, because this surface is tangential to the sunbeams. The flux of direct irradiance over the shaded area, $\Phi_{A_0}(t)$, which might require cumbersome computation if Eq. (13) were used, is also nil, because it results from the difference between two zero terms, that is

$$\Phi_{A_0}(t) = \Phi_{S_0}(t) - \Phi_{A_{0t}}(t) = 0 - 0 = 0 \tag{17}$$

This result holds for all the shaded areas which can occur in the basin, and it leads to the conclusion that the effective average basin flux, $\Phi_{A_e}(t)$ is given simply by the non-shadowing Eq. (11) which is also capable of describing self-shadowing basins. Thus:

$$\Phi_{A_e}(t) = \Phi_A(t) - \Phi_{A_0}(t) = \Phi_A(t) = \boldsymbol{B} \cdot \boldsymbol{R}(t) \tag{18}$$

It should be noted that if the basin is not self-shadowing, the contour, Γ_0, of the shaded area no longer cuts the shaded portion of the basin surface, A_0, from a covering surface which is entirely tangential to the irradiance flux. It follows that Eq. (11) does not hold. However, the deviation of the estimates obtained by using (11) from those obtained by the application of (14) are expected to be minor for most conditions.

5. Application

The performance of (14) has first been compared with that of (4), in estimating clear-sky incoming direct solar radiation over three small catchments. These are the Upper Cordevole basin, the Rio Missiaga experimental catchment, a left-side tributary to Cordevole river, both located in the Eastern Alps of Northern Italy, and the Virginiolo basin, a test site for the MAC EUROPE experiment located in the Appenines of Central Italy, not far from Florence. The Upper Cordevole basin is about 7 km^2 in area with a relief of about 1325 m, ranging from 3152 m (Piz Boè) to 1827 m (Vizza hydrometric station). Topography is described by a rather coarse resolution DEM with a rectangular grid of about 210 × 230 m (Ranzi and Rosso, 1991) The drainage basin of Rio Missiaga is about 4 km^2 in area with a relief of about 1400 m, ranging from 2499 m (Mount Castello) to 1100 m (Rio Missiaga outlet hydrometric station). Topography is described by a fine resolution DEM with elemental cells of 50 × 50 m, obtained by digitising 5-m contours (Mancini et al., 1992). Finally, the Virginiolo basin is a small subcatchment of the Arno river basin with a surface area of about 4 km^2, and a relief of about 175 m. Topography is described by a

fine resolution DEM with elemental cells of 10 × 10 m, obtained by digitising 10-m contours (Mancini et al., 1993).

For the grid integration, averaging was performed by discrete summation of the values taken by $I(u, t)$ and $N_{A(u)}$ for any grid point of the DEM. The same resolution was used for line integration throughout the catchment boundary. Beer's attenuation law is assumed to hold for the exoatmospheric flux, so that the intensity of direct irradiance from the Sun was estimated from

$$I(t) = I_0 e^{-\frac{s}{\sin h(t)}} \tag{16}$$

where I_0 is the solar constant, and s is the optical depth of the atmosphere (see, also, Fouquart et al., 1991).

In Figs. 3, 4 and 5, clear-sky direct radiative flux at the basin scale is plotted against solar azimuth for different values of solar altitude for the three basins investigated. The figures also give the percentage of the basin area that is in shadow, as a function of solar altitude and azimuth angles. The results are also compared in Figs. 6, 7 and 8, where the Stokesian estimates of clear-sky direct radiation are plotted against the grid estimates, i.e. those obtained by the surface integration over the topographic grid. Both methods take shadowing effects into account, since Eqs. (14) and (4) are used, respectively. The deviations of the Stokesian estimates from the spatially distributed ones are negligible. Some very minor deviations could be ascribed to discretisation effects, which may affect grid and contour integrals differently. However, the Stokesian approach, corrected for shadowing, is shown to provide extremely accurate estimates of the global radiative flux due to clear-sky incoming direct solar radiation over the catchments investigated.

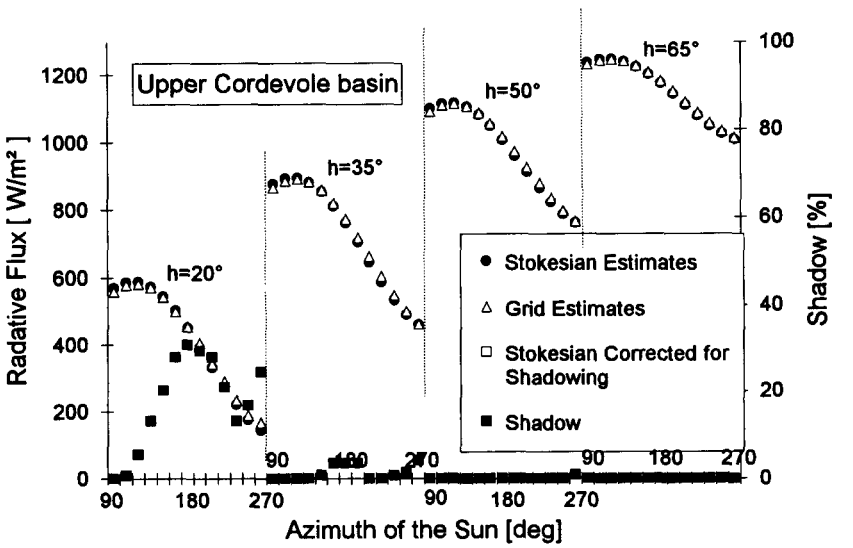

Fig. 3. Estimated clear-sky incoming direct radiation over the Upper Cordevole catchment for different solar geometry.

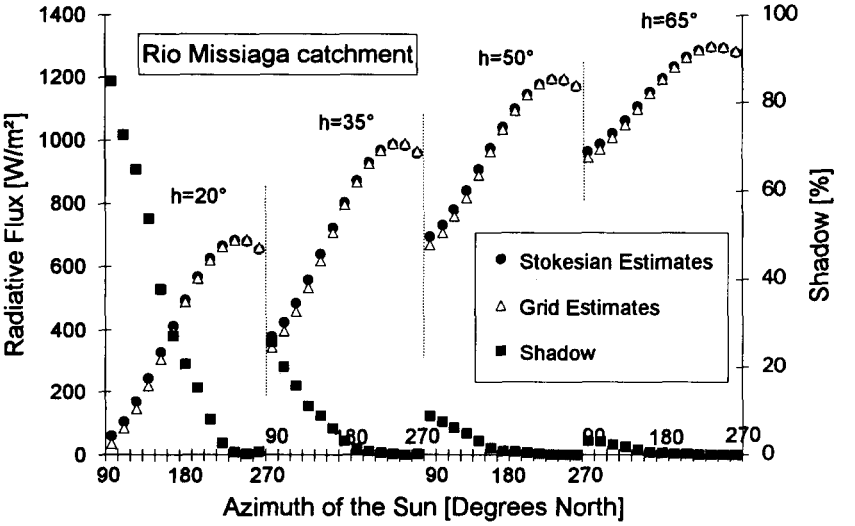

Fig. 4. Estimated clear-sky incoming direct radiation over the Rio Missiaga catchment for different solar geometry.

The performance of the Stokesian method neglecting the effects of shadowing was also investigated, because the use of (11) involves much more straightforward computation than (14). The results are also reported in Figs. 3, 4 and 5 for the three basins investigated. The deviations from the grid estimates are generally minor, as also

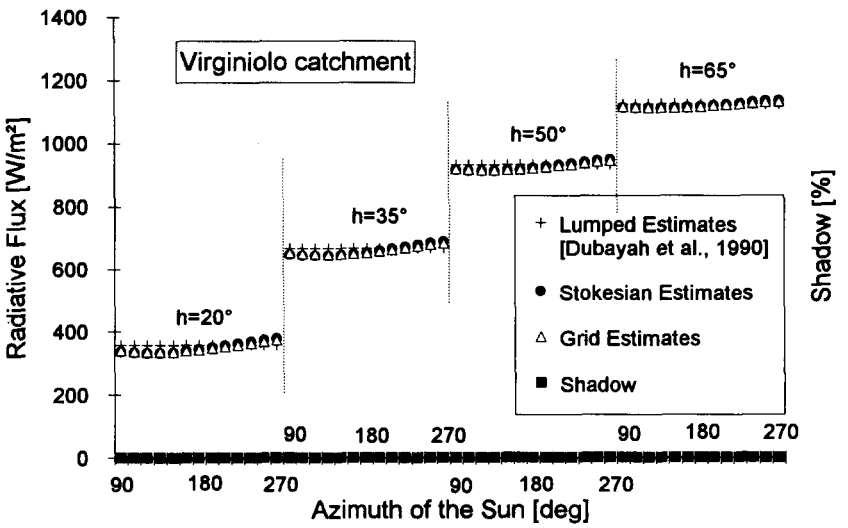

Fig. 5. Estimated clear-sky incoming direct radiation over the Virginiolo catchment for different solar geometry.

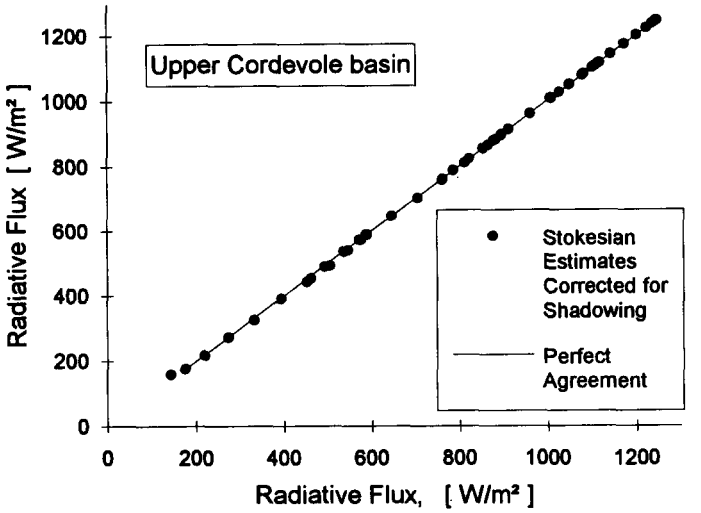

Fig. 6. Stokesian estimates corrected for shadowing vs. grid estimates of clear-sky incoming direct radiation over the Upper Cordevole catchment.

shown in Figs. 9, 10 and 11. The larger deviations are displayed for the Rio Missiaga catchment, where, for some angles of incidence of the solar beam flux, shadows are projected over more than half of the basin area. For the Upper Cordevole basin, minor errors may be induced by the coarse resolution of the DEM, which does not detect shadowing areas with enough accuracy. The Virginiolo catchment is unaffected

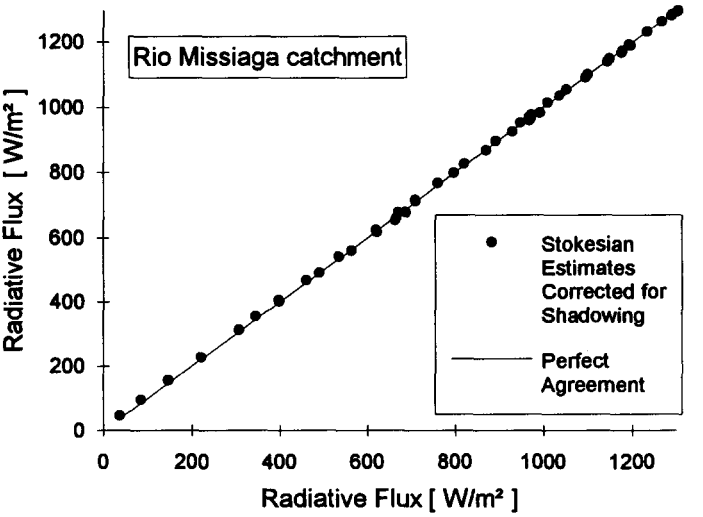

Fig. 7. Stokesian estimates corrected for shadowing vs. grid estimates of clear-sky incoming direct radiation over the Rio Missiaga catchment.

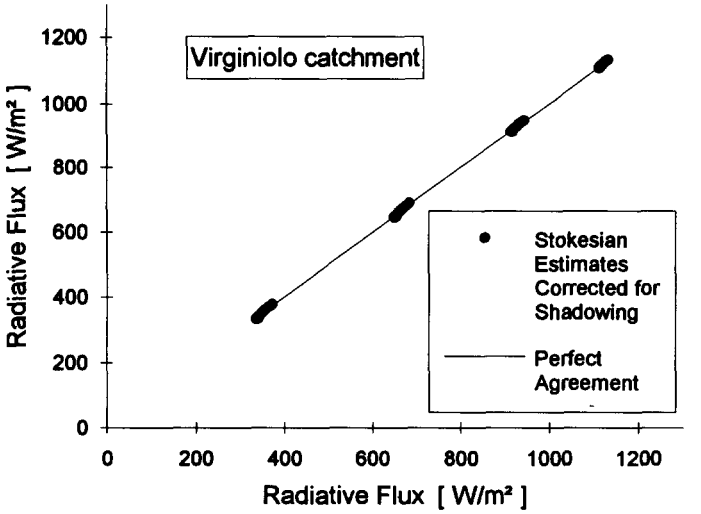

Fig. 8. Stokesian estimates corrected for shadowing vs. grid estimates of clear-sky incoming direct radiation over the Virginiolo catchment.

by shadowing, because its topography slopes gently and shadow does not occur in any of the conditions investigated. However, the effects of shadowing are minor, so that using (11) instead of (14) can provide quite accurate estimates of the global radiative flux owing to clear-sky incoming direct solar radiation over all the catchments investigated. This is true not only when the basins are in self shadowing

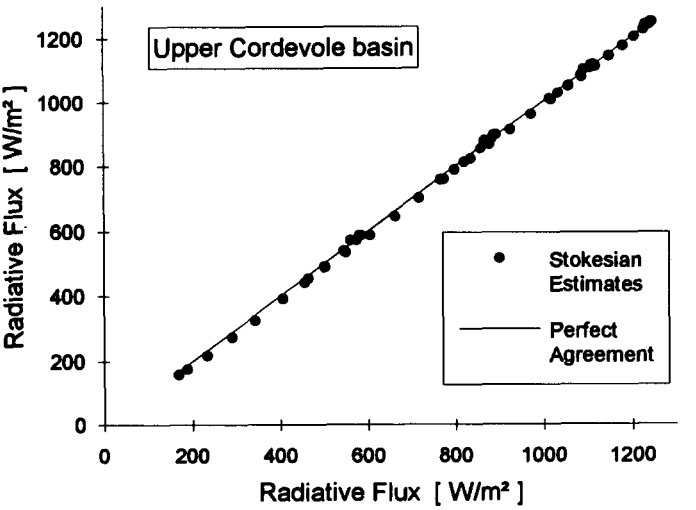

Fig. 9. Stokesian estimates vs. grid estimates of clear-sky incoming direct radiation over the Upper Cordevole catchment.

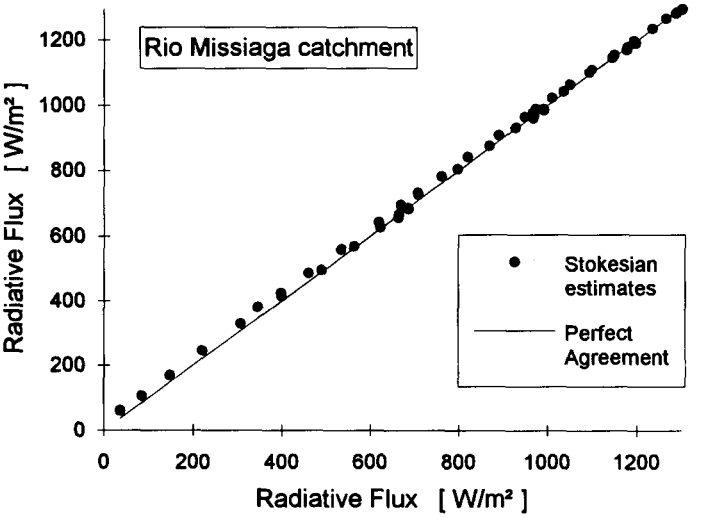

Fig. 10. Stokesian estimates vs. grid estimates of clear-sky incoming direct radiation over the Rio Missiaga catchment.

conditions, but also when the watershed contour projects shadows outside the basin area. This happens, for example, when solar altitude angle is less than 20° in the Rio Missiaga catchment. Therefore, (11) seems to be a suitable candidate for application to hydrological studies because of its simple and meaningful formulation, and its straightforward application.

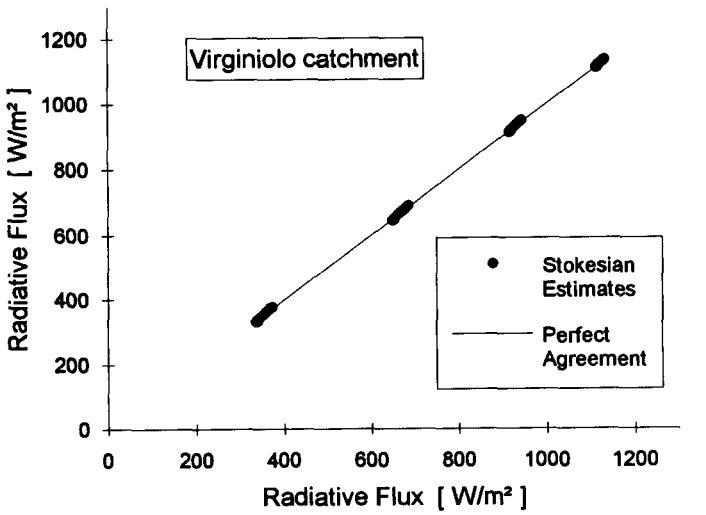

Fig. 11. Stokesian estimates vs. grid estimates of clear-sky incoming direct radiation over the Virginiolo catchment.

Finally, these results have been compared with those achievable by the application of the lumped model used by Dubayah et al. (1990). This model assumes a simplified geometry to describe catchment geomorphology, where slopes are equal, and aspects are uniformly distributed in all directions. Under the above assumption on the intensity of direct irradiance from the Sun, this model yields

$$\Phi_A(t) = I_0 e^{-\frac{s}{\sin h(t)}} \cos S \tag{17}$$

with S denoting the slope of catchment hillslopes. The results are also shown in Figs. 5 and 13 for two of the catchments investigated, i.e. Virginiolo and Rio Missiaga, respectively. This model is not able to represent accurately the effective basin flux for the Rio Missiaga. This is perhaps because of the neglect of the interaction between solar geometry and topography for areas of high relief, where the influence of solar azimuth is significant. However, the results for the Virginiolo basin are satisfactory: a simplified catchment geometry is capable of representing the gentler topography, as displayed by the Virginiolo. The poor performance for mountainous terrain of high relief may be also owing to the underlying assumption of uniformly distributed aspect. This assumption is shown to fit poorly the sampling frequency distribution of aspect for the Missiaga basin (see Fig. 12). Therefore , this model seems to be capable of describing direct solar radiation for basins of moderate relief only.

6. Conclusion

The Stokesian approach to the problem of determining clear-sky radiation for mountainous terrain provides a satisfactory solution, the accuracy of which does not differ significantly from that achievable by means of grid modelling. Although shadowing effects can also be accounted for, the Stokesian solution can provide satisfactory estimates neglecting these effects, and it can be applied easily owing to its simplicity and straightforwardness. Accordingly, clear-sky incoming direct radiation over a drainage basin can be estimated from the scalar product of two vectors. These are the 'shifted beam radiation' vector, which depends on solar geometry only, and the 'topographic boundary' vector, which is dimensionless, and depends on basin topography only, namely the geometry of the catchment boundary. Therefore, this solution accounts separately for the temporal and spatial variability of the process being investigated, and it could be valuable to climatic and hydrological studies. It is shown that the Stokesian solution is analytically correct even when shadows occur over the basin area, provided that the basin is 'self-shadowing', a concept introduced here.

Finally, an alternative lumped model suggested by Dubayah et al. (1990) is found to provide rather unsatisfactory estimates for basins of high relief, while it can be applied to hilly landscapes with minor loss of accuracy. However, this model could also be improved by accounting properly for the effective frequency distribution of aspect, which appears to be far from the uniform assumption

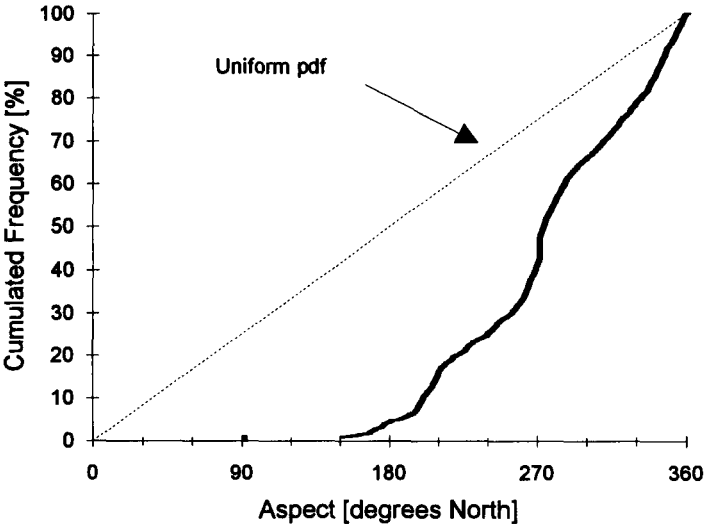

Fig. 12. Sampling cumulated frequency distribution of aspect for the Missiaga catchment as compared with the uniform assumption.

at least for the Missiaga catchment. If a triangular probability density, instead of a uniform one, is assumed for aspect in all directions, the lumped model seems to improve its performance, although the Stokesian approach remains more precise, as shown in Fig. 13. However, looking for an appropriate global description of

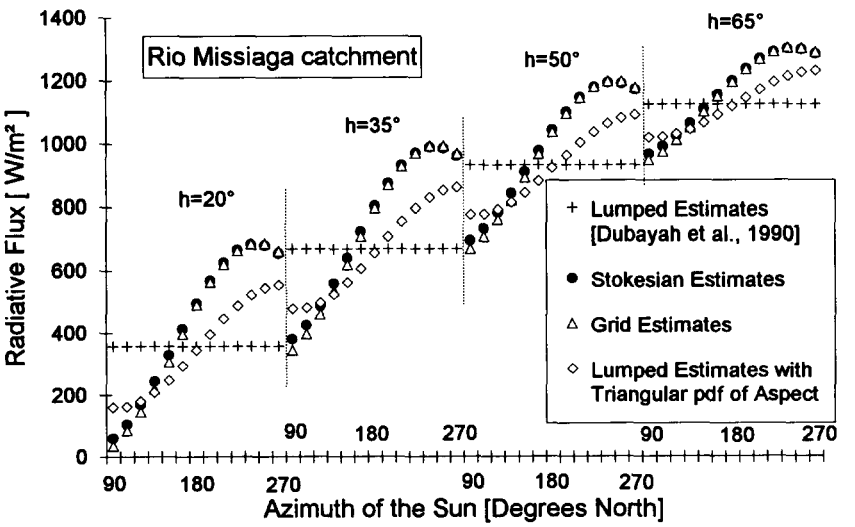

Fig. 13. Estimated clear-sky incoming direct radiation over the Rio Missiaga catchment for different solar geometry.

the interaction between solar geometry and basin topography will require further research efforts.

Acknowledgements

Grateful thanks are expressed to Dr. V. Villi (CNR-IRPI, Padua) for providing the data concerning the Rio Missiaga catchment, to S. Orlandini for DEM processing and to M. Mancini for providing the data for the Virginiolo catchment from the MAC EUROPE experiment. This research was jointly supported by the Ministry for University and Scientific and Technologic Research of Italy through grant MURST 40% 'Processi Idrologici Fondamentali', and by the National Research Council of Italy through the National Group for Prevention from Natural Hazards through Grant CNR92.0144.PF42.

References

Band, L.E., 1989. A terrain based watershed information system. Hydrol. Processes, 3: 151–162.

Band, L.E., 1993. Extraction of channel networks and topographic parameters from digital elevation data. In: K. Beven and M.J. Kirkby (Editors), Channel Network Hydrology, John Wiley and Sons, Chichester.

Burrough, P.A., 1986. Principles of Geographycal Information Systems. Oxford University Press, Oxford.

Demidovich, E. (Editor), 1968. Problems in Mathematical Analysis. Mir, Moscow.

Dozier, J., 1980. A clear-sky spectral solar radiation model for snow-covered mountainous terrain. Water Resour. Res., 16: 709–718.

Dozier, J. and Outcalt, S.J., 1979. An approach toward energy balance simulation over rugged terrain. Geogr. Anal., 11: 65–85.

Dubayah, R., Dozier, J. and Davis, F.W., 1989. The distribution of clear-sky radiation over varying terrain. Proc. Int. Geosci. Remote Sens. Symp., 89: 855–888.

Dubayah, R., Dozier, J. and Davis, F.W., 1990. Topographic distribution of clear-sky radiation over the Konza prairie, Kansas. Water Resour. Res., 26: 679–690.

Fouquart, Y., Bonnel, B. and Ramaswamy, V., 1991. Intercomparing shortwave radiation codes for climate studies. J. Geophys. Res., 96: 8955–8968.

Holland, P.G. and Steyn, D.G., 1975. Vegetational response to latitudinal variations in slope angle and aspect. J. Biogeogr., 2: 179–193.

Isard, S.A., 1983. Estimating potential direct insolation to alpine terrain. Arctic and Alpine Research, 15: 77–89.

Kirkpatrick, J.B. and Nunez, M., 1980. Vegetation–radiation relationships in mountainous terrain. J. Biogeogr., 7: 197–208.

Mancini, M., Orlandini, S. and Rosso, R., 1992. The representation of soil–vegetation–atmosphere at the elemental cell scale in distributed hydrologic models (La rappresentazione del sistema elementare suolo–vegetazione–atmosfera nei modelli idrologici distribuiti), Proc. XXIII Conf. on Hydraulics and Water Engineering, Florence, 31 August–4 September, Vol. 1, pp. 61–78, (in Italian).

Mancini, M., Rosso, R., Lin, D.S., Wood, E. F. and Troch, P., 1993. AIRSAR capability in soil moisture content for different climatic scenarios. Proc. XXV Int. Symp. on Remote Sensing and Global Environmental Change, Graz, 4–8 April, Vol. I, pp. 185–200.

Moore, I.D., Grayson, R.B. and Ladson, A.R. 1991. Digital terrain modelling, A review of hydrological, geomorphological and biological applications. Hydrol. Processes, 5: 3–30.

Ranzi, R. and Rosso, R., 1991. A physically based approach to modelling distributed snowmelt in a small

alpine catchment. In: H. Bergmann, H. Lang, W. Frey, D. Issler and B. Salm (Editors), Snow Hydrology and Forests in High Alpine Areas, IAHS Publ. No. 205, Institute of Hydrology, Wallingford, pp. 141–150.

Ranzi, R. and Rosso, R., 1993. A Stokesian model of areal clear-sky direct radiation for mountainous terrain. Geophys. Res. Lett., 20: 2893–2896.

Williams, L.D., Barry, R.G. and Andrews, J.T., 1972. Application of computed global radiation for areas of high relief. J. Appl. Meteorol., 11, 526–533.

Wood, E.F., Sivaplan M., Beven, K.J. and Band, L., 1988. Effects of spatial variability and scale with implications to hydrologic modelling. J. Hydrol., 102: 29–47.